Journal of the Serbian Chemical Society
JSCS@tmf.bg.ac.rs • www.shd.org.rs/JSCS

J. Serb. Chem. Soc. 74 (4) 427–440 (2009) UDC 536.2:536.7+547.321'212:541.18.045
JSCS–3844 *Original scientific paper*

Local heat transfer coefficients during the evaporation of 1,1,1,2-tetrafluoroethane (R-134a) in a plate heat exchanger

EMILA ŽIVKOVIĆ[1*#], STEPHAN KABELAC[2] and SLOBODAN ŠERBANOVIĆ[1#]

[1]*Faculty of Technology and Metallurgy, University of Belgrade, Karnegijeva 4, 11120 Belgrade, Serbia and* [2]*Helmut Schmidt University of the Federal Armed Forces, Holstenhofweg 85, D-22043 Hamburg, Germany*

(Received 10 June, revised 30 October 2008)

Abstract: The evaporation heat transfer coefficient of the refrigerant R-134a in a vertical plate heat exchanger was investigated experimentally. The area of the plate was divided into several segments along the vertical axis. For each of the segments, the local value of the heat transfer coefficient was calculated and presented as a function of the mean vapor quality in the segment. Owing to the thermocouples installed along the plate surface, it was possible to determine the temperature distribution and vapor quality profile inside the plate. The influences of the mass flux, heat flux, pressure of system and the flow configuration on the heat transfer coefficient were also taken into account and a comparison with literature data was performed.

Keywords: plate heat exchanger; evaporation; R-134a; heat transfer coefficient.

INTRODUCTION

Plate heat exchangers (PHE) have been widely used for almost a century due to their good thermal performance, modest space requirements, easy accessibility to all areas and lower capital and operating costs in comparison to the most commonly used shell-and-tube heat exchangers. In the past, PHE were extensively used in the food and pharmaceutical industries but their application field has expanded to the chemical, petrochemical and process industries. In refineries and petrochemical plants, PHE are applied to many hydrocarbon processes, including catalytic reforming, desulphurization, isomerization, and aromatic recoveries. Typical applications of PHE in the chemical industry are as coolers of acetic acid, sulfuric acid and organic solutions.

Their high thermal performance and compactness made PHE suitable as evaporators or condensers in many refrigeration, air conditioning, and heat pump systems where the fluid acting as the heat source or heat sink is a liquid. For

* Corresponding author. E-mail: emila@tmf.bg.ac.rs
# Serbian Chemical Society member.
doi: 10.2298/JSC0904427Z

these purposes, various refrigerants have been used as working fluids. Serious depletion of the ozone layer in the atmosphere and global warming problems created a need for the development of new refrigerants, such as R-134a, R143a, R-407c, R-410a, R-417a or R-507, with low values of ozone depletion potential (ODP) and global warming potential (GWP). Application of these refrigerants on the other hand required the knowledge of their thermodynamic, thermophysical, and heat transfer properties.

Literature data on two-phase heat transfer, especially for the new refrigerants in PHE, are relatively scarce. In the past years, experimental data for evaporation heat transfer in PHE were published by a few research groups. Experimental investigations on evaporation heat transfer of different refrigerants in PHE are summarized in a previous paper.[1] Yan and Lin[2] explored the evaporation of the refrigerant R-134a in a plate heat exchanger. Their data, used in this study for comparison, produce the local heat transfer coefficient for a 60° chevron type plate as a function of the vapor quality, mass flux and heat flux. A few years later, using the same setup, Hsieh *et al.*[3] investigated the subcooled flow boiling of R-134a, as well as the heat transfer characteristics of the refrigerant R-410a during evaporation[4] and saturated flow boiling processes.[5] The evaporation and condensation of R-134a were also the subject of our previous investigation.[1,6–8] Previously, heat transfer during the boiling process was explored on different plate geometries and with several refrigerants (R-12, R-22, R-113 and R-717) used as the working fluid.[9]

The aim of this work, which is a continuation of our previous investigations,[1,6–8] was to obtain values of the local heat transfer coefficients as a function of vapor quality for different mass and heat fluxes, system pressures and flow configurations. Local temperature measurements along the plate produced temperature profiles and allowed the calculation of vapor distribution along the plate during evaporation.

EXPERIMENTAL

The experimental system used in the present investigation included two vertical PHE – an evaporator and a condenser. It consisted of two main loops, a refrigerant loop and a water––glycol loop, as well as of a data acquisition unit. A detailed description of the experimental setup can be found in a previous paper[1] and a schematic representation of the system is given in Fig. 1. During the experiments, the temperatures, pressures, and flow rates were measured in both loops of the system. The refrigerant loop contained an evaporator (1), separator (2), expansion valve (3), inner heat exchanger (4), compressor (5), two oil separators (6), condenser (7), refrigerant collector with a level indicator (8), two sight glasses and also two volume flowmeters. A vertical plate and a frame heat exchanger was used as the condenser (7). It consisted of 10 plates forming 4 channels for the refrigerant and 5 for the secondary fluid flow, as shown in Fig. 2. Except the two single plates at each end of the stack, the remaining 6 formed 4 double-plate cassettes, inside of which the refrigerant flow passed. The plate characteristics are given in a previous paper[1] and a schematic representation is shown in Fig. 3.

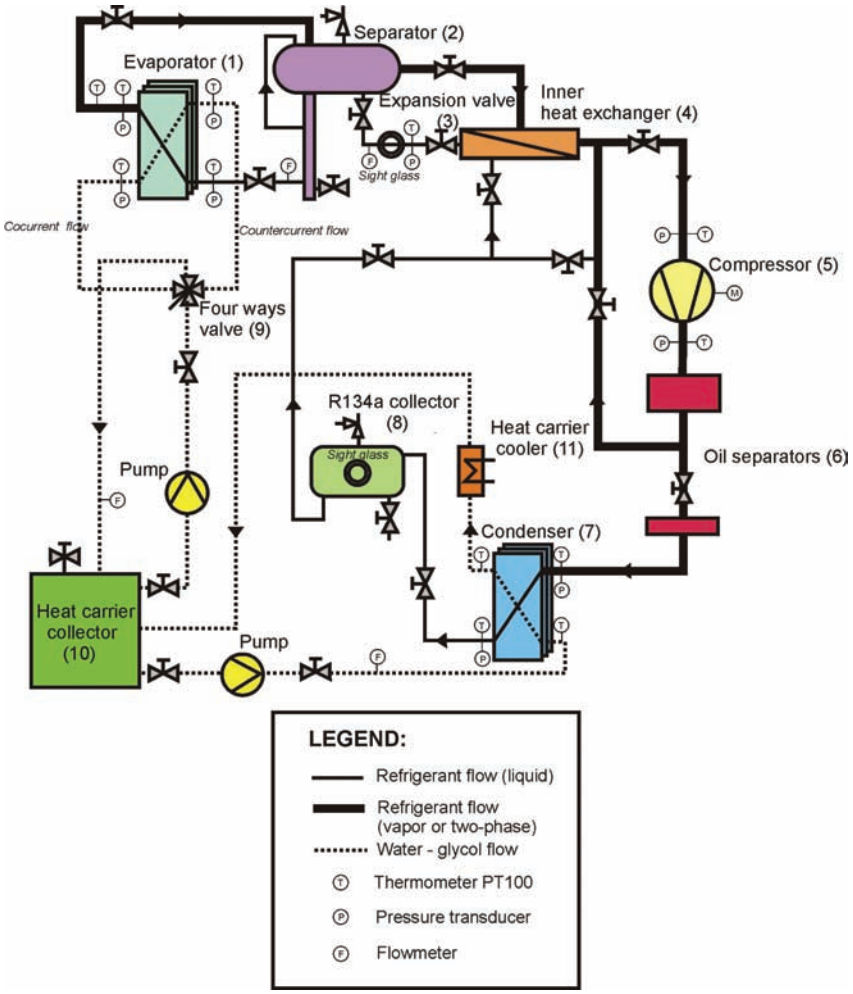

Fig. 1. Experimental setup.

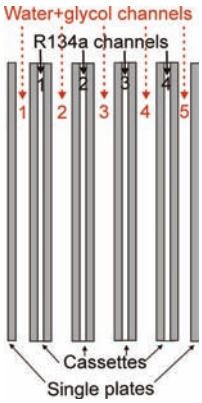

Fig. 2. PHE configuration.

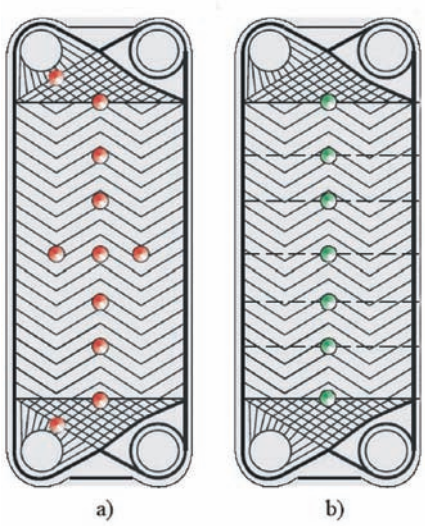

Fig. 3. Plate geometry and thermocouples position; a) wall temperature thermocouples and b) fluid temperature thermocouples.

A special feature of this setup is the measurement of the temperature profile along the plate inside the PHE. Thermocouples (type K, 0.5 mm diameter) were welded along the plate surface in a vertical line on the two middle cassettes for local temperature measurement. The thermocouples were used for measuring the wall temperature on one of the plates and the fluid temperature on the other one, which enabled a direct calculation of local heat transfer coefficients on the water–glycol side. The wall temperature thermocouples were fixed onto the plates *via* small dimples of silver solder, while the fluid temperature thermocouples were fixed a few millimeters below the temperature sensitive head and bent into the middle of the fluid flow channel. The thermocouples were calibrated repeatedly with single phase flow on both sides of the PHE to ensure reliable temperature readings.

In the central horizontal line of the plates, three fluid thermocouples were placed laterally next to each other to check on possible maldistribution within one plate channel. Since their temperature readings agreed within ±1 °C, lateral flow maldistribution seemed to be negligible. Additional thermocouples were installed on each of the remaining two cassettes, at the inlet and at the outlet of the secondary fluid channels, to check on possible maldistribution of the secondary fluid between the plates of the PHE.

Typical temperature profiles along the plate (measured temperatures of the secondary fluid and calculated refrigerant temperatures) are shown in Fig. 4 for concurrent and in Fig. 5 for countercurrent flow. In addition to the measurements by the thermocouples, the temperature of both fluids at the inlet and outlet ports of the condenser were measured by Pt100 resistance thermometers, calibrated against a PTB standard (Physikalish Technische Bundesanstalt Braunschweig, Germany). The differential and absolute pressures were measured using Holox-membrane pressure transducers connected to the inlet and outlet ports of the PHE.

In order to obtain various test conditions, such as the vapor quality at the exit of the evaporator, pressure, flow rate, and imposed heat flux, various water–glycol flow rates were used and the compressor power was changed.

Since the evaporator operated in the thermosyphon mode, the refrigerant mass flux in the evaporator sub-cycle was higher than the mass flux within the loop, thus two flowmeters were required on the refrigerant side. At the evaporator inlet, the volumetric flow rate of the refri-

gerant was measured by a calibrated KROHNE Ultrasonic Flowmeter (type UFM 3030) with an uncertainty of ±1 % and before the expansion valve by a turbine flowmeter, calibrated in--house, with an uncertainty of around 2 %. The water–glycol loop consisted of two sub-cycles, one connected with the evaporator and the other with the condenser. For temperature and pressure measurements of the secondary fluid, Pt100 thermometers and pressure transducers were used at the inlets and outlets of both heat exchangers. The flow rate was measured by a turbine flowmeter with an uncertainty of ±1.5 % in the evaporator sub-cycle and by a TRIMEC Multipulse Positive Displacement MP025 flowmeter with an uncertainty of ±0.5 % in the condenser subcycle. The resistance thermometers, the pressure transducers, and the flowmeters were calibrated repeatedly.

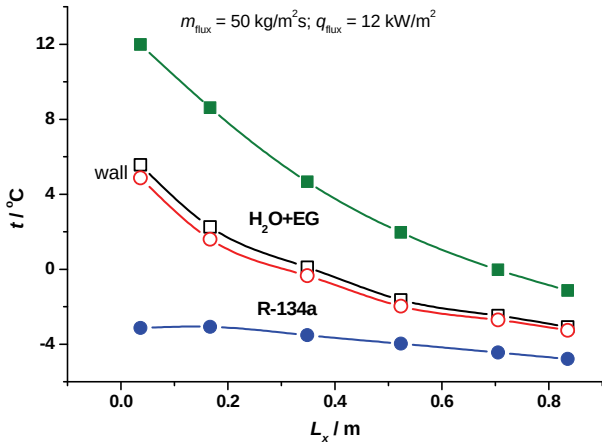

Fig. 4. Temperature profiles of R-134a and the ethylene glycol + water mixture (EG + H_2O) along the plate for concurrent flow.

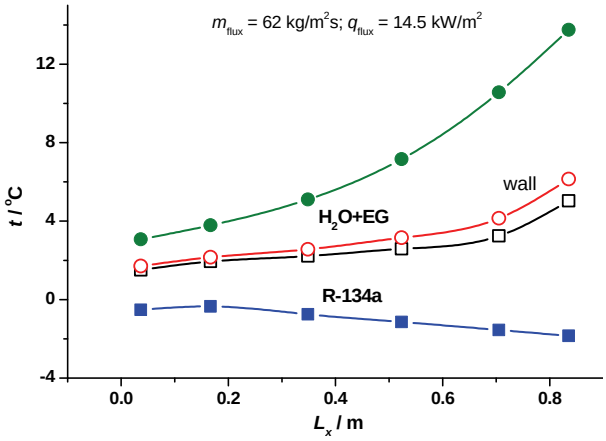

Fig. 5. Temperature profiles of R-134a and the ethylene glycol + + water mixture (EG + H_2O) along the plate for countercurrent flow.

The data acquisition system included a recorder (KETHLEY 2750 Multimeter), a power supply, and a personal computer. The temperature and voltage data were recorded and the collected data signals were then transmitted through a GPIB interface to a computer for further analysis. The experiment was monitored and controlled, and a preliminary balance check was realized by a routine written in the LabVIEW® program.

For calculation purposes, the plate area was divided into several segments along the vertical axis, on the borders of which thermocouples were installed on the cooling liquid side (Fig. 3). The energy balance for each of the segments was checked and the amount of heat transferred calculated. Since the heat transfer coefficients were calculated separately for each segment of the plate, they represent local values.

For every segment of the plate, the heat flux between the two fluids, q_x, was calculated using the water–glycol side data:

$$q_x = m_{\mathrm{h,c}} c_{p,\mathrm{h}} (T_{\mathrm{h},x,\mathrm{i}} - T_{\mathrm{h},x,\mathrm{o}}) / A_x \tag{1}$$

where $m_{\mathrm{h,c}}$ is the mass flow rate of the heating fluid through one channel and $T_{\mathrm{h},x,\mathrm{i}}$ and $T_{\mathrm{h},x,\mathrm{o}}$ are the inlet and outlet temperatures for one segment on the water–glycol side, respectively.

The area of the segment available for heat transfer, A_x, was calculated from the equation:

$$A_x = 2 L_x B_\mathrm{p} \Phi \tag{2}$$

where L_x is the length of the segment, B_p the plate width and Φ the area enhancement factor.

The local heat transfer coefficients for the single phase water–glycol mixture, $\alpha_{\mathrm{h},x}$ were determined as:

$$\alpha_{\mathrm{h},x} = \frac{q_x}{T_{\mathrm{h},x} - T_{\mathrm{w,h},x}} \tag{3}$$

The mean values of the fluid temperature, $T_{\mathrm{h},x}$, and wall temperature, $T_{\mathrm{w,h},x}$, in each segment, from the heating liquid side, were calculated from the measured inlet and outlet temperatures. Wall temperature from the refrigerant side, $T_{\mathrm{w,r},x}$, can be expressed as:

$$T_{\mathrm{w,r},x} = T_{\mathrm{w,h},x} - \frac{q_x \delta_\mathrm{p}}{\lambda_\mathrm{p}} \tag{4}$$

where δ_p and λ_p are the plate thickness and the thermal conductivity of the plate material, respectively.

Finally, local heat transfer coefficients, $\alpha_{\mathrm{r},x}$, were determined from the equation:

$$\alpha_{\mathrm{r},x} = T_{\mathrm{w,h},x} - \frac{q_x}{T_{\mathrm{w,r},x} - T^\mathrm{s}_{\mathrm{r},x}(p^\mathrm{s}_{\mathrm{r},x})} \tag{5}$$

where $T^\mathrm{s}_{\mathrm{r},x}$ is the refrigerant evaporation temperature, determined as a function of the saturation pressure, $p^\mathrm{s}_{\mathrm{r},x}$.

The saturation pressures at the chosen positions along the plate, $p^\mathrm{s}_{\mathrm{r},x}$, were calculated with an uncertainty of less than 10 % from the measured overall pressure drop.

Heat released from the heating fluid was partly used for heating the refrigerant to the saturation point, $q_{\mathrm{r,s,sens}}$, and partly for evaporation, $q_{\mathrm{r,s,lat}}$:

$$q_x = q_{\mathrm{r,s,sens}} + q_{\mathrm{r,s,lat}} \tag{6}$$

$$q_{\mathrm{r},x,\mathrm{sens}} = (T^\mathrm{s}_{\mathrm{r,x}} - T_{\mathrm{r,i}}) m_{\mathrm{r,c}} c_{p,\mathrm{r}} / A_x \tag{7}$$

$$q_{\mathrm{r},x,\mathrm{lat}} = m_{\mathrm{r,c}} \Delta h_\mathrm{v} \Delta x / A_x \tag{8}$$

In Eqs. (6)–(8), $m_{\mathrm{r,c}}$, represents the mass flow rate of the refrigerant through one channel, $T_{\mathrm{r,i}}$ is the refrigerant temperature and Δh_v is the specific enthalpy of vaporization.

Since the sub-cooling of the refrigerant was very small, usually a few degrees, the evaporation process began in the first segment of the plate. In this segment, both terms in Eq. (6)

were taken into account. In all of the following segments, the heat transferred to the refrigerant was used only for evaporation.

The change in the refrigerant vapor quality, Δx, was calculated from Eq. (9):

$$\Delta x = \frac{q_{\mathrm{r},x,\mathrm{slat}} A_x}{m_{\mathrm{r,c,h}} \Delta h_{\mathrm{v}}} \tag{9}$$

An uncertainty analysis was conducted on the basis of a procedure suggested by Moffat.[10] In the cases where a quantity, for example a heat transfer coefficient, could not be directly measured, it could be calculated from a set of measurements using a data fitting program represented by

$$y = f(x_1, x_2, x_3, \ldots x_N) \tag{10}$$

The directly measured variables, $(x_1, x_2, x_3, \ldots x_N)$ were presented in the following form:

$$x_i = x_{i,\mathrm{exp}} + u(x_i) \tag{11}$$

where $x_{i,\mathrm{exp}}$ is the measured value and $u(x_i)$ is the uncertainty based on specific probability.

The uncertainty in the calculated result has to be expressed with the same probability as that used in the estimation of the uncertainties in the measurements. According to Kline and McClintock,[11] the uncertainty in a calculated variable could be estimated with good accuracy using a root-sum-square combination of the effects of each of the individual inputs

$$u(y) = \sqrt{\sum_i \left(\left(\frac{\partial f}{\partial x_i} \right)_{x_{j \neq i}} u(x_i) \right)^2} \tag{12}$$

If the calculation from Eq. (12) involves an expression that is difficult to differentiate, the numerical approach may be used.[10]

For calculation purposes, Eq. (12) was transformed into a more suitable form:

$$u(y) = \sqrt{\sum_i \left(\frac{f(x_i + \delta) - f(x_i - \delta)}{2\delta} u(x_i) \right)^2} \tag{13}$$

where δ is the uncertainty interval.

More details on uncertainty analysis, calculation procedures and possible sources of uncertainties are given in literature.[12] The uncertainties of the thermophysical properties, as well as the uncertainties of the instrumentation, were taken into account and the evaluation results are summarized in Table I.

TABLE I. Estimated uncertainties

Parameter	Uncertainty	
	Relative	Absolute
Geometry of the plates		
Length, width and thickness	±1.5 %	$\pm 5\times10^{-5}$ m
Area	±4.5 %	$\pm 7\times10^{-5}$ m^2
Measuring instruments		
Temperature, PT100	±1.5 %	±0.1 °C
Temperature, TC	±5 %	±0.4 °C
Pressure transducers	±1 %	±200 Pa

TABLE I. Continued

Parameter	Uncertainty	
	Relative	Absolute
Water flowrate – turbine	±1.5 %	±1.0 min^{-1}
Water flowrate – multipulse positive displacement flowmeter	±0.5 %	±0.35 min^{-1}
R134 flowrate – ultrasonic flowmeter	±1 %	±0.15 min^{-1}
R134 flowrate – turbine	±2 %	±0.3 min^{-1}
Evaporation heat transfer		
Heat flux	±7.5 %	±1.7 kW m^{-2}
Vapor quality	±8.5 %	±0.05
Heat transfer coefficient	±15 %	±400 W m^{-2} K^{-1}

RESULTS AND DISCUSSION

A series of experiments on R-134a evaporation in a vertical PHE were conducted under different test conditions. The evaporation temperature was varied from –8.85 to 11.08 °C (saturation pressure from 0.21 to 0.43 MPa), the values of the refrigerant mass flux were between 40 and 90 kg m^{-2} s^{-1} and the corresponding values of the heat flux were from 9 to 15 kW m^{-2}. The experiments involved both concurrent and countercurrent flow of fluids through the evaporator. The working conditions of pressure, mass flux, heat flux and flow configuration during the experiments presented in this paper are summarized in Table II. The

TABLE II. Working conditions during the experiments

Name	Flow configuration	No. of compressor cylinders	Pressure MPa	Heat flux kW/m^2	Mass flux kg/m^2 s
LTEST 1	Concurrent	2	0.33–0.38	9	50
LTEST 2		2			60
LTEST 3		2			75
LTEST 4		2		10	50–55
LTEST 4a	Countercurrent	2			
LTEST 5	Concurrent	2			60
LTEST 5a	Countercurrent	2			
LTEST 6	Concurrent	2			65–70
LTEST 7		2			75–80
LTEST 8	Countercurrent	2			85
LTEST 9	Concurrent	2	0.38–0.44	10	55–60
LTEST 10		2			75–80
LTEST 11		2		11	55–60
LTEST 12		2			60–65
LTEST 13	Concurrent	4	0.25–0.27	12	45–50
LTEST 14	Countercurrent	4		13.5	60–70
LTEST 15	Concurrent	4	0.27–0.30	14.5	50–60
LTEST 15a	Countercurrent	4		14.5	

thermophysical properties of R134-a, necessary for the calculation of the local heat transfer coefficients and pressure drops, were taken from the REFPROP database.[13] The calculated values of the local heat transfer coefficients and pressure drop in each of the segments are graphically presented as functions of the mean vapor quality in the segment. The mean vapor quality, x_m, is the average vapor quality in the segment, estimated from the inlet value x_i and the vapor quality change Δx.

Influences of the refrigerant mass flux, heat flux, system pressure and flow direction on the evaporation heat transfer were analyzed closely. The influence of mass flux on the heat transfer coefficient in the case of concurrent flow is illustrated in Fig. 6. The heat transfer coefficient increases with increasing mass flux, more significantly for higher vapor quality, which would indicate the dominance of the convective boiling regime. A similar dependency is shown in Fig. 7 for the case of countercurrent flow. This tendency could be explained by the fact that with a higher vapor quality, the liquid film on the plate surface is thinner and since this film represents an additional resistance to heat transfer, the resulting effect on the heat transfer coefficient becomes favorable. This behavior is, however, contrary to the usual assumption that for small and medium vapor qualities, nucleate boiling is dominant, hence, the heat transfer coefficient is independent of mass flux and vapor quality. It should be noted here that these local values do

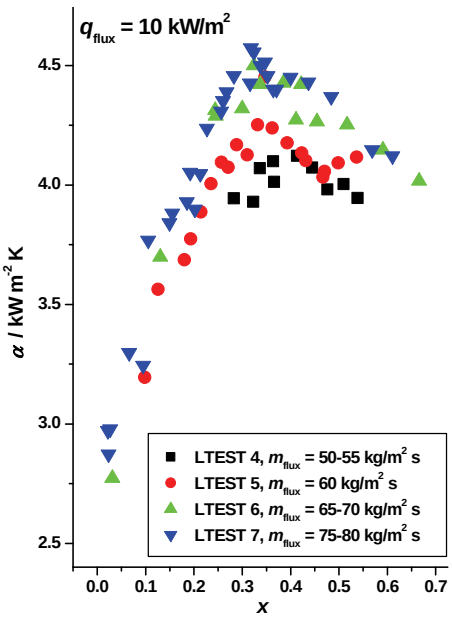

Fig. 6. Influence of mass flux on the heat transfer coefficient; concurrent flow.

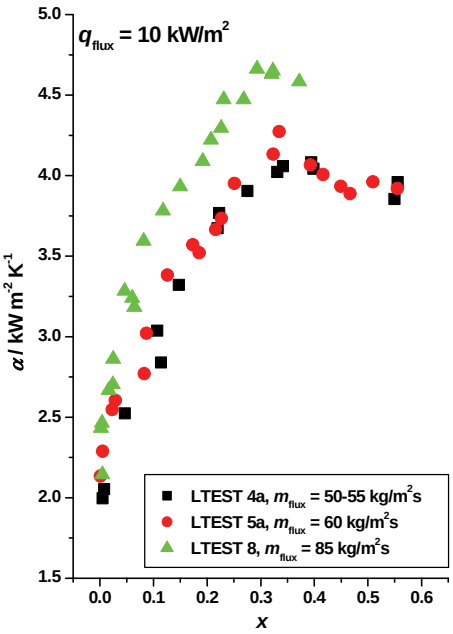

Fig. 7. Influence of mass flux on the heat transfer coefficient, countercurrent flow.

not correspond to the succeeding values along the plate length within one specific run. As the heat flux changes significantly along the plate, the results presented in Figs. 6–8 and 11–12 have been sorted into groups of similar mass and heat fluxes in order to be comparable.

The effect of heat flux on the heat transfer coefficient is shown in Fig. 8 for three heat fluxes, keeping the mass flux and system pressure constant. An increase in the heat flux induces an increase in the heat transfer coefficient, although the effect is not as significant as in the previous case of the influence of mass flux. For smaller heat and mass fluxes, the heat transfer coefficient seems to remain constant, or even slightly drop, after reaching the maximum value, as can be seen in Figs 6–8. A similar behavior was also noticed earlier.[12] For higher values of heat flux (Fig. 8, q_{flux} = 14.5 kW m^{-2}), this tendency does not seem to appear.

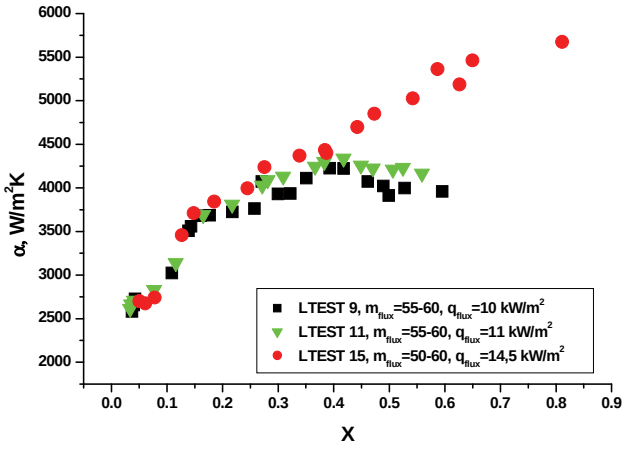

Fig. 8. Influence of heat flux on the heat transfer coefficient.

Concurrent and countercurrent flows are compared and analyzed in Figs. 9 and 10. The concurrent flow seems to give a more than 10 % higher heat transfer coefficient and higher outlet vapor quality than the countercurrent flow, under similar working conditions. In Fig. 10, the vapor quality is shown as a function of the plate position for two countercurrent flow cases and the corresponding concurrent flow cases. The vapor quality increases more quickly in the case of the concurrent flow, as a result of larger temperature difference at the entrance, as can be seen in Fig. 4.

The last analyzed parameter is the system pressure, which exhibits only a smaller influence on the heat transfer coefficient, as can be seen in Fig. 11.

The results of the series of measurements under various experimental conditions are compared with literature data[2] in Fig. 12. Although the measurements of Yan *et al.*[2] were conducted in a PHE of different geometry, satisfactory agreement was achieved.

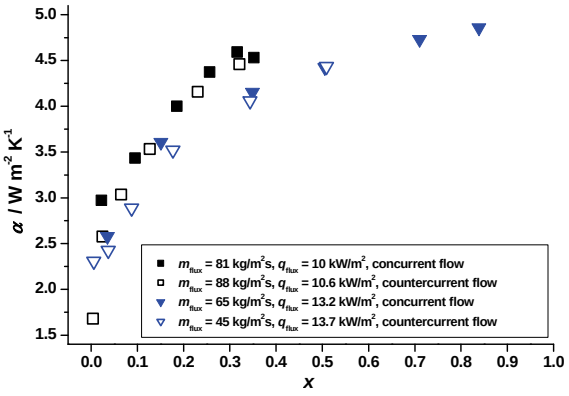

Fig. 9. Influence of flow configuration on the heat transfer coefficient.

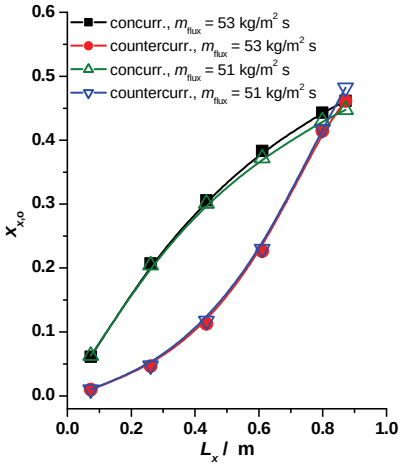

Fig. 10. Evolution of the local vapor quality along the plate for the concurrent and countercurrent flow configurations.

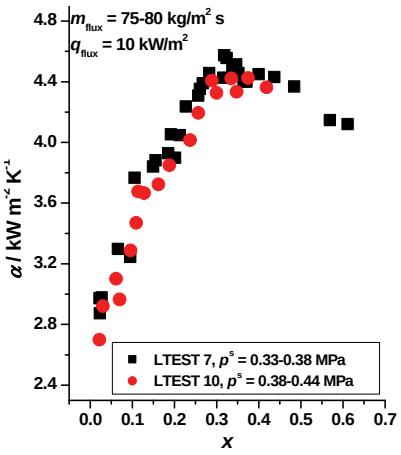

Fig. 11. Influence of system pressure on the heat transfer coefficient.

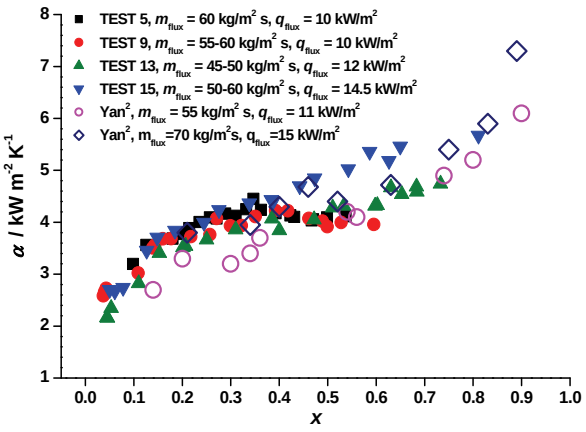

Fig 12. Comparison with previous experimental data.[1]

CONCLUSIONS

The effects of the refrigerant mass flux, heat flux, vapor quality, system pressure and flow configuration on the evaporation heat transfer coefficient were investigated and discussed. A special feature of the employed experimental setup was the measurement of temperature profiles along the plates inside the PHE, which allowed the calculation of local values of the heat transfer coefficient as a function of the vapor quality. As a result of the investigation, the following conclusions can be drawn:

– increasing the vapor quality induces an increase in heat transfer coefficient during R-134a evaporation;

– increasing the refrigerant mass flux and the imposed heat flux results in a better evaporation heat transfer coefficient, although the effect of the heat flux seems to be less significant;

– the question of the dominant boiling mechanism remains unresolved. It seems that convective boiling is dominant, at least for the smaller values of heat flux. More data are required to clarify the limits and the overlap of the relevant boiling mechanisms;

– the concurrent flow configuration gives higher values of the heat transfer coefficient than the countercurrent flow configuration, due to the higher temperature differences between both fluids and faster rise in vapor quality in the entrance region.

NOTATIONS

A	Heat transfer area, m^2
B_p	Width, m
c_p	Specific heat, $J/kg^{-1}\ K^{-1}$
L	Length, m
m	Mass flow rate, kg/s
m_{flux}	Mass flux, $kg/m^{-2}\ s^{-1}$
p^s	Saturation pressure, Pa
q	Heat flux, W/m^2
T	Temperature, K
T^s	Saturation temperature, K
T_w	Wall temperature, K
Δh_v	Specific enthalpy of vaporization, J/kg
$u(y)$	Measurement uncertainty
x	Mean vapor quality

Greek letters

α	Heat transfer coefficient, $W/m^{-2}\ K^{-1}$
δ_p	Thickness of the plate, m
Φ	Area enhancement factor due to corrugation
λ_p	Thermal conductivity of plate material, W/m K
ψ	Angle of plate corrugation, deg.

Subscripts

c Channel
i Inlet
h Hot water-glycol mixture
o Outlet
p Plate
r Refrigerant
x Segment

Acknowledgements. The experimental investigation presented in this paper was conducted in the Laboratory of the Institute of Thermodynamics at the Helmut Schmidt University of the Federal Armed Forces in Hamburg, Germany. The setup was partially supported by GEA Ecoflex GmbH, Sarstedt, Germany. The research visit of the first author in Hamburg was financed by the German Academic Exchange Bureau, DAAD. The results reported in this study are also a part of the scientific project financed by the Ministry of Science and Technological Development of the Republic of Serbia.

ИЗВОД

ЛОКАЛНИ КОЕФИЦИЈЕНТИ ПРЕЛАЗА ТОПЛОТЕ ПРИ ИСПАРАВАЊУ 1,1,1,2-ТЕТРАФЛУОРЕТАНА (R-134a) У ПЛОЧАСТОМ РАЗМЕЊИВАЧУ ТОПЛОТЕ

ЕМИЛА ЖИВКОВИЋ[1], STEPHAN KABELAC[2] и СЛОБОДАН ШЕРБАНОВИЋ[1]

[1]*Технолошко–металуршки факултет, Универзитет у Београду, Карнегијева 4, 11120 Београд и*
[2]*Helmut Schmidt Univerzitet u Hamburgu, Holstenhofweg 85, D-22043 Hamburg, Germany*

У овом раду је експериментално испитиван коефицијент прелаза топлоте при двофазном току расхладног флуида 1,1,1,2-тетрафлуороетана (R-134a) у вертикалном плочастом размењивачу топлоте. Површина плоче је подељена у неколико сегмената дуж вертикалне осе. У сваком од сегмената израчуната је локална вредност коефицијента прелаза топлоте и приказана у функцији средњег степена сувоће у сегменту. Захваљујући термопаровима постављеним дуж површине плоче, било је могуће одредити температурне профиле и расподелу степена сувоће дуж плоче. Испитивани су утицаји масеног флукса, топлотног флукса, радног притиска и конфигурације тока флуида на коефицијент прелаза топлоте и извршено је поређење са одговарајућим литературним подацима.

(Примљено 10. јуна, ревидирано 30. октобра 2008)

REFERENCES

1. E. Đorđević, S. Kabelac, S. Šerbanović, *J. Serb. Chem. Soc.* **72** (2007) 833
2. Y. Y. Yan, T. F. Lin, *ASME J. Heat Transfer* **121** (1999) 118
3. Y. Y. Hsieh, L. J. Chiang, T. F. Lin, *Intern. J. Heat Mass Transfer* **45** (2002) 1791
4. Y. Y. Hsieh, T. F. Lin, *ASME J. Heat Transfer* **125** (2003) 852
5. Y. Y. Hsieh, T. F. Lin, *Int. J. Heat Mass Transfer* **45** (2002) 1033
6. E. Đorđević, S. Kabelac, S. Šerbanović, *J. Serb. Chem. Soc.* **72** (2007) 1015
7. E. Đorđević, S. Kabelac, S. Šerbanović, *Chem. Pap.* **62** (2008) 78
8. E. Đorđević, S. Kabelac, *Int. J. Heat Mass Transfer* **51** (2008) 6235
9. R. Osterberger, B. Slipccevic, *Ki Klima – Kälte – Heizung* **11** (1990) 481
10. R. J. Moffat., *Exp. Therm. Fluid Sci.* **1** (1988) 3
11. S. J. Kline, F. A. McClintock, *Mechan. Eng.* **75** (1953) 3

12. M. Andre, *PhD Thesis*, Hannover University, Germany, 2004
13. M. O. McLinden, S. A. Klein, E. W. Lemmon, A. P. Peskin, *NIST thermodynamic and transport properties of refrigerant mixtures – REFPROP*, Version 6.0, NIST, Boulder, 1998.